



PROF. RAMON MERINO (Orcid ID : 0000-0002-5306-0635)

Article type : Full Length

Article type: Full Length

## **Therapeutic effects of anti-Bone Morphogenetic Protein and Activin Membrane-Bound Inhibitor treatment in psoriasis and arthritis.**

Pilar Alvarez, PhD,<sup>1</sup> Juan Jesús Agustín, PhD,<sup>2,\*</sup> Esther Tamayo, PhD,<sup>2,\*</sup> Marcos Iglesias, PhD,<sup>2</sup> Olga Acinas, MD,<sup>3</sup> M<sup>a</sup> Angeles Mendiguren, MD,<sup>4</sup> José Andrés Vázquez, MD,<sup>4</sup> Fernanda Genre, PhD,<sup>2</sup> David San Segundo, PhD,<sup>5</sup> Jesús Merino, MD, PhD,<sup>2,\*\*</sup> and Ramón Merino, MD, PhD,<sup>1,2,\*\*</sup>.

<sup>1</sup>Instituto de Biomedicina y Biotecnología de Cantabria, Consejo Superior de Investigaciones Científicas-Universidad de Cantabria-SODERCAN, Santander, Spain; <sup>2</sup>Departamento de Biología Molecular-IDIVAL Universidad de Cantabria, Santander, Spain; <sup>3</sup>Servicios de Anatomía Patológica, <sup>4</sup>Radiofísica y Protección Radiológica and <sup>5</sup>Inmunología, Hospital Universitario Marqués de Valdecilla, Santander, Spain.

**Keywords:** BAMBI, Psoriasis, Arthritis, Tregs, TGF $\beta$

**Running head:** Anti-BAMBI therapy in autoimmunity

\*These authors contribute equally to this work.

\*\*These authors share senior authorship.

This article has been accepted for publication and undergone full peer review but has not been through the copyediting, typesetting, pagination and proofreading process, which may lead to differences between this version and the [Version of Record](#). Please cite this article as [doi: 10.1002/ART.41272](https://doi.org/10.1002/ART.41272)

This article is protected by copyright. All rights reserved

**Address Correspondence:** Dr. Ramón Merino, Instituto de Biomedicina y Biotecnología de Cantabria, C/ Albert Einstein 22, PCTCAN, 39011 Santander, Spain.

Phone: 34 942 206855; e-mail: merinor@unican.es

**Funding:** Funding was provided by grants from the Spanish Ministerio de Economía y Competitividad (Plan Nacional I+D+i) co-financed by European Development Regional Fund to RM (SAF2017-82905-R) and JM (SAF2016-75195-R). PA and MI were partially supported by grants from “Luchamos por la Vida Foundation” and the Spanish Ministerio de Economía y Competitividad (IPT2011-1527-010000) associated with Fibrostatin SL, respectively.

**Conflict of interest:** JM and RM are cofounders and stockholders of Inhibitec-Anticuerpos S.L. that possessed the license for the commercialization and exploitation of a patent application entitled “Monoclonal antibodies against BAMBI and use for the treatment of inflammatory diseases”. The other authors declare no conflict of interest.

## Abstract

**Objectives:** Transforming growth factor beta (TGF $\beta$ ) inhibitor Bone Morphogenetic Protein and Activin Membrane-Bound Inhibitor (BAMBI) has been shown to control CD4<sup>+</sup> T lymphocytes differentiation into either tolerogenic regulatory T (Tregs) or pathogenic T<sub>H</sub>17 cells through the regulation of TGF $\beta$  and IL-2 signaling strength. In the present study, we explore the potential beneficial effects of its pharmacological inhibition with new anti-BAMBI monoclonal antibodies (mAbs) in different skin and joint experimental chronic-inflammatory/autoimmune diseases.

**Methods:** Development of *saccharomyces cerevisiae* mannan-induced psoriatic arthritis (MIP) (n= 18-30 mice/group), imiquimod-induced skin psoriasis (n= 20-30 mice/group) or collagen type II-induced arthritis (CIA) (n= 13-16 mice/group) was analyzed in a total number of 2-5 different experiments with B10.RIII wild type (WT) or BAMBI-deficient mice treated or not with B101.37 (mouse IgG1 anti-BAMBI), mouse IgG1 anti-TNP isotype control, anti-CD25 or anti-TGF $\beta$  mAbs.

**Results:** Treatment of normal mice with an IgG1 anti-BAMBI mAb, clone B101.37, expands Tregs in vivo and has both preventive and therapeutic effects in the murine model of MIP (p<0.05 in both cases). Disease protection is mediated by Tregs, which control the activation and expansion of pathogenic IL-17-producing cells, and is dependent on TGF $\beta$ . Furthermore, B101.37 treatment blocks the development of skin psoriasis induced by imiquimod and of CIA (p<0.05 in both cases). Finally, the pharmacological inhibition of BAMBI with the IgM anti-BAMBI B143.14 mAb also potentiates the suppressive activity of Tregs in vitro (p<0.001).

**Conclusions:** We identify BAMBI as a promising new therapeutic target for chronic-inflammatory diseases and other pathological conditions modulated by Tregs.

## Introduction

Regulatory CD4<sup>+</sup> T cells (Tregs) exhibit suppressive properties and their absence and/or abnormal function promote autoimmune diseases (1-5). Tregs also prevent allograft rejection (6). Therefore, therapeutic strategies aimed to increase their numbers and/or activity are currently under investigation in different clinical trials (7, 8). Tregs can be subdivided into thymus-derived Tregs, which differentiate within the thymus from immature T cells, and peripheral Tregs, derived from CD4<sup>+</sup> T cells activated in secondary lymphoid organs in the presence of transforming growth factor  $\beta$  (TGF $\beta$ ) and IL-2 (1, 2, 9).

TGF $\beta$  also participates in the conversion of CD4<sup>+</sup> T lymphocytes into T<sub>H</sub>17 cells (10-12), a subpopulation of effector cells involved in the defense against extracellular bacteria and fungi (13), but also in many inflammatory diseases (14). The capacity of TGF $\beta$  to promote the differentiation of T<sub>H</sub>17 cells depends on the co-presence in the environment of pro-inflammatory cytokines such as IL-6, IL-23, IL-1 $\beta$  and/or IL-21 (10-12, 15, 16). In addition, we have recently reported that BAMBI (**B**one Morphogenetic Protein and **A**ctivin **M**embrane-**B**ound **I**nhibitor) regulates the activity of TGF $\beta$  during T<sub>H</sub>17/Treg differentiation (17).

BAMBI is a transmembrane protein homologous to TGF $\beta$  type I receptors (T $\beta$ RI) that antagonizes TGF $\beta$  superfamily signals by preventing the formation of active receptor complexes upon ligand binding (18). We have demonstrated that BAMBI fixes the intensity of TGF $\beta$  signaling and regulates CD25 expression and IL-2 signaling strength in CD4<sup>+</sup> T lymphocytes. Consequently, BAMBI deficiency increases and decreases the *in vitro* and *in vivo* Treg and T<sub>H</sub>17 differentiation, respectively (17). These results point to this pseudoreceptor as a new potential therapeutic target in chronic-inflammatory diseases. Here, we have explored this possibility by evaluating the preventive and therapeutic effects of the treatment with a new anti-BAMBI monoclonal antibody (mAb) in the development of several murine experimental chronic-inflammatory skin and joint diseases.

## Methods

### Mice and mAbs.

C57BL/6 wild type (B6.WT) and B10.RIII.WT mice were obtained from Charles River (Barcelona, Spain). The generation of B6 mice deficient in BAMBI (B6.BAMBI-KO) and B10.RIII.BAMBI-KO mice has been described recently (17). All experimental disease models

were performed in 2-3 months-old B10.RIII male mice, using control littermates in the experiments with BAMBI-KO. Mice were maintained in a conventional animal room at the University of Cantabria animal facilities. Genotyping of mice was performed by PCR of genomic tail DNA. For bone marrow (BM) chimeras, 2 months-old B10.RIII.WT and B10.RIII.BAMBI-KO male mice were irradiated uniformly at 950 cGy with a dose rate of 130 cGy/min and reconstituted with  $10^7$  BM cells (BMC) from either B10.RIII.WT or B10.RIII.BAMBI-KO mice. The level of hematopoietic reconstitution was controlled by flow cytometry two months later. All animal care and experimental procedures were approved by the Universidad de Cantabria Institutional Laboratory Animal Care and Use Committee (ref 2017/05).

B101.37 (mouse IgG1) and B143.14 (mouse IgM) anti-BAMBI mAbs were described previously (17). Anti-TGF $\beta$  (clone 1D11, mouse IgG1) and anti-CD25 (clone PC61, rat IgG1) mAbs were obtained from the ATCC (LGC Standards S.L.U., Barcelona, Spain). The MM17F3 mAb, which produced a murine IgG1 anti-mouse IL-17A mAb (19), was a kind gift from Dr. Jacques Van Snick (Ludwig Institute for Cancer Research, Brussels, Belgium) and the murine IgG1 anti-TNP isotype control mAb (IgG1-C) was kindly provided by Prof. Shozo Izui (Department of Pathology and Immunology, University of Geneva, Switzerland).

### **Induction and assessment of chronic-inflammatory diseases and treatments.**

In all experimental models, the clinical severity and histological scores were determined by two blinded observers. For the induction of *Saccharomyces cerevisiae* mannan (SCM) psoriatic arthritis (PsA) (MIP), WT IgG1-C or B101.37 treated, BAMBI-KO and BM chimeric mice were injected intraperitoneally (ip) with 10 mg of SCM (Sigma–Aldrich) dissolved in 200  $\mu$ l of PBS, either only on day 0 or for multiple exposures additionally on days 7 and 14, as described previously (20). The severity of skin psoriasis was evaluated daily by measuring ear thickening using a digital caliper (Somet CZ, Bilina, Czech Republic), macroscopically at the end of the experiment and then again after histological analysis of paraffin-embedded tissue sections stained with hematoxylin and eosin (H&E). Paw swelling was scored daily, as described previously (17, 21). At the end of the experiment hind paws were fixed in 10% phosphate-buffered formaldehyde solution, decalcified in Parengy's decalcification solution overnight and paraffin-embedded tissue sections (4  $\mu$ m) were stained with H&E. Gene expression of IL-1 $\beta$ , TNF $\alpha$ , IL-6, IL-17A and IL-23 cytokines in the ears and hind paws was explored 6 days after PBS or SCM injection by means of

quantitative real time RT-PCR, as described previously (21). Results (in triplicate) were normalized to *GAPDH* expression and measured in parallel in each sample.

Imiquimod-induced skin psoriasis was induced after topical application of a cream containing 5% imiquimod (Aldara®, 3M pharmaceuticals) for five consecutive days (12.5 mg imiquimod/day) on the right ears of IgG1-C or B101.37 treated WT or BAMBI-KO male mice. Left ears were kept untreated as controls. The severity of psoriasis was evaluated daily by analyzing erythema and desquamation according to a graded scale from 0 to 3 as follows: 0=normal skin; 1=small changes; 2=moderate changes; 3=big changes. In addition, ear thickening in imiquimod-treated ears was evaluated in comparison to their respective untreated control ears using a digital caliper and graded from 0 to 4 as follows: 0=no thickening; 1=1-10% of increase; 2=10-25% of increase; 3=26-50% of increase; 4=>50% of increase. The scores of these individual aspects of dermatitis were added to obtain the cumulative score. Imiquimod-treated and control ears were analyzed by histology at the end of the experiment. Sections (4 µm) of paraffin-embedded tissues were stained with H&E. For epidermal and dermal thickening quantification, images from 3 different sections in each ear were captured and quantified with an Axio Scan Z1 equipped with the ZEN 2012 (blue edition) software (Zeiss Iberica, Madrid, Spain). Thickening was evaluated in 3 different ear regions at each cartilage side (total 6 measurements/section/mice). Total values represent the mean of the individual 18 measurements per ear.

Bovine col II (MD Bioproducts, Zürich, Switzerland) was emulsified with complete Freund's adjuvant (CFA) containing 4 mg/ml of *Mycobacterium tuberculosis* (MD Bioproducts). The induction of CIA in IgG1-C or B101.37 treated WT and BAMBI-KO males and the clinical and radiological evaluation of arthritis severity was performed as described previously (17, 21). Sections of paraffin-embedded hind paws were stained with H&E. Synovial inflammation, bone erosion, cartilage damage, and leukocyte infiltration were assessed in at least 4 different sections using a scale of 0–4 (normal = 0; mild = 1; moderate = 2; marked = 3; severe = 4). Histological score was calculated by summation of these scales.

B6.BAMBI-KO and B6.WT mice treated with IgG1-C or B101.37 mAbs were injected with JES6-1A12 containing IL-2-anti-IL-2 immune complexes (IL-2 IC) as previously described (22). The effects on Tregs in lymph nodes and spleen were evaluated 5 days later by flow cytometry.

For in vivo inhibition of BAMBI, mice were treated ip with 2 mg/week of B101.37 or IgG1-C mAbs. Control mice were treated with 2 mg/week of IgG1-C mAb. For CD4<sup>+</sup>CD25<sup>+</sup> cell depletion, WT and BAMBI-KO mice were treated ip with 1 mg of anti-CD25 mAb one week before SCM injection. For in vivo TGFβ or IL-17 inhibition, WT and BAMBI-KO mice were injected with 1 mg of the respective mAb the day before SCM injection.

### **Cell cultures.**

Naïve CD4<sup>+</sup> and Treg cells from B6.WT mice were purified by cell sorting on a FACSaria (BD Biosciences, Madrid, Spain). Antigen presenting cells (APCs) were obtained from irradiated spleen cells. For the assessment of Treg activity, 5x10<sup>4</sup> CD4<sup>+</sup>CD25<sup>-</sup> cells were cultured in triplicate over 3 days in complete RPMI medium and stimulated with 0.5 μg/ml of anti-CD3 mAb in the presence of 5x10<sup>4</sup> APCs, decreasing ratios of Tregs and 20 μg/ml of IgM anti-BAMBI B143.14 mAb or 20 μg/ml of murine IgM (Sigma, St Louis, Missouri). Cultures were pulsed with 1 μCi of <sup>3</sup>H-methyl-thymidine (<sup>3</sup>H-TdR) for the final 6 h of culture, harvested and counted.

### **Flow cytometry.**

Frequencies of Treg and T<sub>H</sub>17 cells in spleen, lymph nodes and ears were explored in IgG1-C or B101.37 treated WT and BAMBI-KO mice by flow cytometry using commercially labeled antibodies 6 days after PBS or SCM injection (Biolegend and eBioscience). Intracellular cytokine staining was performed using an intracellular staining kit (BD Biosciences) as described previously (17, 21). For ear cell suspensions, pools from 3-5 ears/experimental groups were obtained. Skin sheets from the naïve and diseased mouse ears were separated from cartilage and processed as described earlier (23). Cells were analyzed in a FACSCanto II flow cytometer using FACSDiva software (BD Biosciences).

### **Statistics.**

Statistical differences were analyzed by one way and two-way ANOVA, with Tukey's or Dunnett's multiple comparison test and by Student's t test using the GraphPad® Prism 6.0 software. Probability values <0.05 were considered significant.

## **Results**

## **Pharmacological inhibition of BAMBI with anti-BAMBI mAbs enhances in vivo Treg expansion and increases their in vitro suppressive activity.**

We recently described the generation of two mouse anti-mouse BAMBI mAbs, clones B101.37 (mouse IgG1) and B143.14 (mouse IgM) (17). Here, we explored the in vivo inhibitory activity of B101.37 mAb. Treatment of B6.WT mice with B101.37 caused a slight but significant increase in the percentage of Tregs in lymph nodes and spleen when compared to B6.WT mice receiving IgG1-C (Figure 1A and Supplementary Table 1). As previously reported (17), the injection of IL-2 IC containing the JES6-1A12 mAb, which selectively targeted T cells expressing CD25 (22), promoted a greater expansion of Tregs in the lymph nodes and spleen of B6.BAMBI-KO than in B6.WT mice (Figure 1A and Supplementary Table 1). Interestingly, the increase in Tregs caused by IL-2 IC in B6.WT mice was also higher after B101.37 mAb treatment than after IgG1-C injection (Figure 1A and Supplementary Table 1).

Tregs from B6.BAMBI-KO mice exhibited higher expression of CD25 than those of B6.WT mice (17) (Figure 1B). Treg expression of CD25 in B6.WT mice increased after treatment with B101.37 mAb to the levels found in untreated B6.BAMBI-KO mice and higher than in IgG1-C-treated WT mice, regardless of IL-2 IC injection (Figure 1B and Supplementary Table 1).

Our previous findings showed that BAMBI deficiency also enhanced the in vitro suppressive activity of Tregs (17). Accordingly, the suppressive activity of B6.WT Tregs was increased after the addition of B143.14 mAb to the cultures, which inhibited BAMBI in vitro (17), but not of an IgM isotype control antibody (Figure 1C). Altogether, these results indicated that BAMBI inhibition with B101.37 or B143.14 mAbs caused the expansion of Tregs in vivo and increased their suppressive potential in vitro, respectively.

### **Effect of BAMBI deficiency or its pharmacological inhibition with B101.37 mAb in MIP.**

Since B101.37 mAb inhibited BAMBI and expanded Tregs in vivo, we explored its potential therapeutic effect in a recently described experimental murine model of PsA named MIP (20). Following a single ip injection of 10 mg of SCM, susceptible B10.RIII.WT mice treated with IgG1-C developed an inflammatory disease affecting the skin and paws that reached its maximum score 4-5 days later (Figure 2A and Supplementary Table 2). Macroscopically, the ears and footpads of these animals presented signs of a psoriasis-like skin disease such as erythema, scaling, and thickening (Figure 2B-C). Histologically, the diseased ears showed hyperkeratosis, acanthosis, intracorneal pustules and intense inflammatory infiltrates in the dermis (Figure 2B).



Despite the presence of an evident macroscopic hind paw swelling (Figure 2C), no histological signs of joint inflammation were found in these B10.RIII.WT controls (Supplementary Figure 1). However, pads from SCM injected B10RIII.WT mice showed psoriatic-like skin and localized periostitis lesions (Supplementary Figure 1). Furthermore, a mild increase in Achilles tendon thickening without signs of inflammatory cell infiltration was observed in these mice [(Supplementary Figure 1); SMC/IgG1-C B10RIII.WT:  $199.5 \pm 14.8 \mu\text{m}$  (n=6); SMC/B101.37 B10RIII.WT:  $101.5 \pm 34.8 \mu\text{m}$  (n=6); SMC B10RIII.BAMBI-KO:  $147.5 \pm 10.6 \mu\text{m}$  (n=6);  $p < 0.05$ ], in agreement with that described previously in other strain of mice after SCM injection (20). Remarkably, an intense reduction in the severity of macroscopic and histological skin and paw lesions were observed in B10.RIII.BAMBI-KO mice and in B10.RIII.WT mice treated with B101.37 mAb from the time of SCM injection (Figure 2A-C, Supplementary Table 2 and Supplementary Figure 1).

BAMBI-KO mice exhibited a general BAMBI deficiency (24) and the administration of B101.37 mAb might also cause a widespread inhibition of this pseudoreceptor in WT mice. Therefore, the reduced disease severity observed in protected mice could be due to the absence/inhibition of BAMBI in immune cell populations directly involved in the pathogenesis of this process and/or in other cell types controlling the activity of these relevant immune cells. To discriminate between these two possibilities, lethally irradiated B10.RIII.BAMBI-KO and B10.RIII.WT mice were reconstituted with  $10^7$  BMC from either B10.RIII.BAMBI-KO or B10.RIII.WT mice (Figure 3A). The development of MIP was studied in the different BM chimeras two months later. As observed in non-chimeric mice (Figure 2A), WT→WT and BAMBI-KO→BAMBI-KO chimeras developed either a severe or a mild MIP, respectively (Figure 3B). Interestingly, BAMBI-KO→WT chimeric mice also failed to develop an aggressive disease. In contrast, a similar severe MIP was observed in WT→BAMBI-KO and WT→WT chimeras (Figure 3B), indicating that the development or protection against MIP in the different groups of chimeric mice correlated with the phenotype of donor BMC.

To further explore the mechanism of disease protection in B10.RIII.BAMBI-KO and B101.37-treated B10.RIII.WT mice, the expression pattern of mRNAs encoding for different pro-inflammatory cytokines was explored in the ears and hind paws of these animals. A reduced expression of IL-6, TNF $\alpha$ , IL-17A and IL-23 in the ears and of IL-1 $\beta$ , IL-6 and IL-17A in the hind paws was observed in these protected animals in comparison to IgG1-C-treated B10.RIII.WT

controls (Figure 2D). TNF $\alpha$  expression was also reduced in the hind paws of B10.RIII.BAMBI, but not in B101.37-treated B10.RIII.WT mice (Figure 2D).

The pattern of cytokine expression described above was suggestive of an impaired T<sub>H</sub>17 cell activity in protected mice. To analyse this hypothesis and the potential role of Tregs in such protection, changes in the distribution of Tregs and T<sub>H</sub>17 cells were evaluated after MIP induction. Enhanced and reduced expansions of Tregs and T<sub>H</sub>17 cells were observed, respectively, in lymph nodes, spleen (Figure 2E and Supplementary Table 3) and ears (Figure 2F-G) of B10.RIII.BAMBI-KO and B101.37-treated B10.RIII.WT mice after SCM injection in comparison to IgG1-C-treated B10.RIII.WT controls. Furthermore, the depletion of CD4<sup>+</sup>CD25<sup>+</sup> Tregs with a cytotoxic anti-CD25 mAb prior to disease induction, promoted the development of MIP in otherwise protected B10.RIII.BAMBI-KO and B101.37-treated B10.RIII.WT mice (Figure 3C-D and Supplementary Table 4). Interestingly, in vivo blockade of IL-17A with an anti-IL-17A mAb (19) restored the protection against MIP in CD4<sup>+</sup>CD25<sup>+</sup> Treg-depleted B10.RIII.BAMBI-KO and B101.37-treated B10.RIII.WT mice (Figure 3E and Supplementary Table 5), stressing the involvement of IL-17A-producing cells in disease development in Treg-depleted mice.

In addition to TGF $\beta$ , BAMBI negatively regulates Activin and BMP activities (18) and potentiates Wnt signaling (25). However, the administration of an anti-TGF $\beta$  mAb, which selectively inhibits TGF $\beta$  without affecting Activin, BMP or Wnt- $\beta$  catenin signaling pathways, induces the development of MIP in B10.RIII.BAMBI-KO and B101.37-treated B10.RIII.WT mice (Figure 3C-D and Supplementary Table 4).

### **B101.37 treatment exhibits both preventive and therapeutic effects in chronic MIP.**

It has been previously demonstrated that the disease induced after a single injection of SCM is self-limited, but that multiple injections cause a sustained disease (20). We use this chronic variant of the MIP model to evaluate whether the B101.37 treatment possesses not only preventive, but also therapeutic effects in this process. In addition, we explore whether a single injection of B101.37 mAb at the time of disease induction promotes persistent tolerance and blocks long-term disease development. As previously described (20), a weekly ip injection of SCM into IgG1-C-treated B10.RIII.WT mice causes a chronic skin psoriasis and paw swelling (Figure 4). The severity of these manifestations is significantly reduced in B10.RIII.WT mice treated with B101.37 from the time of the first SCM injection up to the end of disease surveillance (preventive regimen; Figure 4). Although a single injection of B101.37 at the time of disease

induction significantly delays the development of MIP, the long-term evolution of the disease is similar to that of IgG1-C-treated B10.RIII.WT mice (Figure 4). The initiation of a maintained B101.37 treatment 3 days after the first SCM injection, when both skin inflammation and paw swelling are already evident (therapeutic regimen), controls the evolution of the disease to a similar extent than in B10.RIII.WT mice receiving a preventive B101.37 treatment (Figure 4).

### **B101.37 treatment prevents imiquimod-induced skin psoriasis and CIA development.**

Our previous results clearly show that BAMBI plays an active role modulating Treg and T<sub>H</sub>17 differentiation during the development of MIP and that the treatment with the inhibitory B101.37 mAb exhibits both preventive and therapeutic effects in this chronic-inflammatory disease. To further support these conclusions, and since no experimental models of psoriasis reproduce all the characteristics of the disease observed in humans (26), we explore the effects of BAMBI deficiency or its pharmacological inhibition with B101.37 in a second experimental model of skin psoriasis; the imiquimod-induced psoriasis (27). Topical application of a cream containing 5% imiquimod for five consecutive days on the right ears of IgG1-C-treated B10.RIII.WT mice induces an inflammatory skin disease (Figure 5 and Supplementary Table 6) with histological features of psoriasis (Figure 5B). The absence of BAMBI in mutant mice or the treatment of WT mice with B101.37 significantly reduces clinical and histopathological signs of disease in these animals (Figure 5 and Supplementary Table 6).

Furthermore, treatment of B10.RIII.WT mice with B101.37 during the first 4 weeks after immunization with col II-CFA inhibited the development of CIA to the same extent as in B10.RIII.BAMBI-KO mice (Figure 6A and Supplementary Table 6). In contrast, B10.RIII.WT mice treated with IgG1-C developed a severe CIA (Figure 6A and Supplementary Table 6). The attenuated disease observed in B10.RIII.BAMBI-KO and B101.37-treated B10.RIII.WT mice was further confirmed by radiological analysis of different signs associated with aggressive arthritis and by histology showing the presence of cartilage and bone destruction, synovitis and pannus formation in the joints of B10RIII.WT, but not of B101.37-treated B10.RIII.WT and B10RIII.BAMBI-KO mice (Figure 6B-C and Supplementary Table 7).

### **Discussion**

BAMBI has been identified as part of a rheostat-like machinery involved in the control of Tregs and T<sub>H</sub>17 differentiation. Its deficiency inhibits the development of CIA, indicating that this molecule could be a novel therapeutic target in chronic-inflammatory/autoimmune diseases (17).

In the present study, we describe the *in vivo* inhibitory activity of a mouse IgG1 anti-BAMBI mAb, clone B101.37. Treatment with this mAb expands Tregs and reduces T<sub>H</sub>17 cells, showing both preventive and therapeutic effects in different experimental murine models of psoriasis and arthritis by Treg and TGF $\beta$ -dependent mechanisms.

Multiple clinical trials have been or currently are in progress to explore the benefits of Treg cell-based therapies in humans (7, 8). However, the protocols employed to purify and *in vitro* expand these cells in sufficient numbers must deal with important technical challenges that have not yet been sufficiently solved. One promising approach consists of the *in vivo* expansion of this cell population using IL-2-IC targeting cells expressing the high affinity IL-2R, such as Tregs (22). This approach has already been employed successfully in the clinic in different pathologies (28-30). Here, we show that the combined administration of IL-2-IC with BAMBI inhibitors such as B101.37 mAb improves this type of Treg therapy. Furthermore, we demonstrate here that the blockade of BAMBI with mAbs potentiates the inhibitory activity of murine Tregs, at least *in vitro*. Altogether, these evidences encourage the possibility of using BAMBI inhibitors for the *in vivo* or *in vitro* Treg expansion protocols in humans.

Using two different murine models of psoriasis associated or nor with paw inflammation and the model of CIA, we demonstrate here that the treatment with B101.37 mAb possesses beneficial effects on these chronic-inflammatory/autoimmune diseases. Since B101.37 mAb is an IgG1, these therapeutic effects are unrelated with a complement-dependent depletion of cells expressing BAMBI (31). In addition, the expansion of Tregs observed after B101.37 treatment and the fact that BAMBI expression is induced after the activation of CD4<sup>+</sup> T cells (17), argues against the possibility of an antibody-dependent cellular cytotoxicity mechanism in such mAb effects. Instead, we postulate that the B101.37 effects are directly associated with the functional inactivation of BAMBI in cells expressing it. In this regard, the extracellular part of BAMBI, the region recognized by B101.37, influences the capacity of the T $\beta$ RI receptor to form homodimers, a process which is required for TGF $\beta$  signaling (18).

The cellular mechanisms accounting for the *in vivo* therapeutic effects of B101.37 have been explored in detail in the model of MIP. Our studies with BM chimeras clearly show that the therapeutic effects of B101.37 mAb are mediated by BM derived cells and not by other cell populations such as keratinocytes potentially involved in disease development (32-34). Furthermore, we demonstrate here that Tregs mediate the protection against the development of MIP in both BAMBI-KO and B101.37-treated WT mice, in agreement with the inhibition of CIA

development in BAMBI-KO mice (17). Recently, Tregs have been shown to control the severity of imiquimod-induced psoriasis by inhibiting the production of type I interferon by mononuclear phagocytes and by suppressing the infiltration of granulocyte-macrophage colony-stimulating factor producing CD4<sup>+</sup> T cells into the lesioned skin (35, 36). Our present results show that in correlation with the reduced disease severity, the absence or pharmacological inhibition of BAMBI promotes a higher increase in the number of Tregs found in different locations, including the skin, than of those found in untreated WT mice. These Tregs control the activity of T<sub>H</sub>17 cells and/or other components of the T17 immune axis. In this regard, disease development observed in BAMBI-KO and B101.37-treated WT mice after Treg depletion with anti-CD25 mAb is blocked after inhibition of IL-17A. The reduced numbers of T<sub>H</sub>17 cells in the spleen, lymph nodes and skin of BAMBI-KO and B101.37-treated WT mice can suggest that these cells may be crucial targets of Treg activity. However, MIP development has been shown to be αβ T-cell-independent (20). Thus, the protective effect of Tregs may be secondary to the control of other IL-17-producing immune cells with a potential role in disease development, such as IL-17-producing γδ T cells and/or ILC3 cells (37).

We have previously reported that BAMBI deficiency increases Treg numbers through the control of CD25 expression and of IL-2 signaling strength by a Smad-3 dependent mechanism (17). The increase in the expression of CD25 in Tregs and in their proliferative responses to IL-2 IC observed in WT mice after treatment with B101.37 indicates that this may also be the mechanism through which this anti-BAMBI mAbs operates in Tregs. Additionally, we show here that BAMBI inhibition modulates MIP development through a TGFβ-dependent mechanism. This is particularly relevant since BAMBI also inhibits BMP an Activin pathway and potentiates Wnt-β catenin signaling (18, 25). The role of TGFβ in psoriasis development is controversial. TGFβ possesses anti-proliferative effects in keratinocytes and promotes their maturation (38, 39). Furthermore, a decrease in TGFβ2, TGFβ3 and Smad-2 expression has been reported in psoriatic skin lesions (40), and the clinical improvement of psoriatic lesions after treatment with methotrexate is associated with an increase in the expression of TGFβ1 (41). On the other hand, an increase in circulating levels of TGFβ1 has been associated with a severe disease (42) and transgenic mice overexpressing TGFβ1 in keratinocytes develop skin psoriasis (43-45). The reason for the apparent discrepancies between these studies and our observations is probably related to the cell type in which BAMBI inhibition alters TGFβ signaling during the development

of MIP. In this regard, the absence of BAMBI in non-hematopoietic cells does not appear to affect disease development in chimeric mice.

In the initial description of the MIP model, it was demonstrated that disease severity was greatly dependent on the strain of mice analyzed and that only B10Q mice with a mutation in the *Ncf1* gene, which caused a reduction in macrophage reactive oxygen species production, developed histological joint lesions (20). In the present work we employed mice in the B10RIII genetic background and despite the presence of an evident macroscopic paw swelling in IgG1-C-treated control WT mice, no histological signs of joint destruction were observed after SCM injection. However, paw swelling in these controls could be attributed to the co-presence of psoriatic-like skin lesions with periostitis and a discrete Achilles tendon thickening. The severity of all these histological lesions was significantly lower in either BAMBI-KO mice or in WT mice after the pharmacological blockade of BAMBI with B101.37 mAb. Furthermore, the beneficial effects of B101.37 in CIA development, clearly emphasized the effects of this treatment not only in chronic-inflammatory skin lesions but also in autoimmune arthritis development.

Multiple mAbs against cytokines or soluble receptors for these factors are used for the treatment of chronic-inflammatory/autoimmune diseases (46, 47). These compounds are very specific and the results obtained with them have been very positive. However, approximately 30% of patients with severe diseases remain unresponsive to existing therapies and the appearance of drug resistances is frequent (48, 49). Our present results describe a potential new molecular target candidate, BAMBI, and new mAb against it, the B101.37 mAb. Experiments are in progress to determine whether B101.37 mAb also modulates BAMBI activity in humans.

### **Acknowledgments**

We thank Drs Jacques Van Snick (Ludwig Institute for Cancer Research, Brussels, Belgium) and Shozo Izui (Department of Pathology and Immunology, University of Geneva, Switzerland) for the MM17F3 and IgG1-C mAbs, respectively. We also thank María Aramburu and Iván Gómez for technical assistance.

### **References**

1. Josefowicz SZ, Lu LF, Rudensky AY. Regulatory T cells: mechanisms of differentiation and function. *Annu Rev Immunol.* 2012;30:531-64.

2. Kitagawa Y, Sakaguchi S. Molecular control of regulatory T cell development and function. *Curr Opin Immunol.* 2017;49:64-70.
3. Fontenot JD, Gavin MA, Rudensky AY. Foxp3 programs the development and function of CD4<sup>+</sup> CD25<sup>+</sup> regulatory T cells. *Nat Immunol.* 2003;4:330-6.
4. Fontenot JD, Rasmussen JP, Williams LM, Dooley JL, Farr AG, Rudensky AY. Regulatory T cell lineage specification by the forkhead transcription factor Foxp3. *Immunity.* 2005;22:329-41.
5. Hori S, Nomura T, Sakaguchi S. Control of regulatory T cell development by the transcription factor Foxp3. *Science.* 2003;299:1057-61.
6. Hall BM. CD4<sup>+</sup>CD25<sup>+</sup> T regulatory cells in transplantation tolerance: 25 years on. *Transplantation.* 2016;100:2533-47.
7. Sharabi A, Tsokos MG, Ding Y, Malek TR, Klatzmann D, Tsokos GC. Regulatory T cells in the treatment of disease. *Nat Rev Drug Discov.* 2018;17:823-44.
8. Tang Q, Vincenti F. Transplant trials with Tregs: perils and promises. *J Clin Invest.* 2017;127:2505-12.
9. Chen W, Jin W, Hardegen N, Lei KJ, Li L, Marinos N, et al. Conversion of peripheral CD4<sup>+</sup>CD25<sup>-</sup> naive T cells to CD4<sup>+</sup>CD25<sup>+</sup> regulatory T cells by TGF- $\beta$  induction of transcription factor *Foxp3*. *J Exp Med.* 2003;198:1875-86.
10. Bettelli E, Carrier Y, Gao W, Korn T, Strom TB, Oukka M, et al. Reciprocal developmental pathways for the generation of pathogenic effector TH17 and regulatory T cells. *Nature.* 2006;441:235-8.
11. Mucida D, Park Y, Kim G, Turovskaya O, Scott I, Kronenberg M, et al. Reciprocal TH17 and regulatory T cell differentiation mediated by retinoic acid. *Science.* 2007;317:256-60.
12. Veldhoen M, Hocking RJ, Atkins CJ, Locksley RM, Stockinger B. TGF $\beta$  in the context of an inflammatory cytokine milieu supports de novo differentiation of IL-17-producing T cells. *Immunity.* 2006;24:179-89.
13. Chen Z, O'Shea JJ. Th17 cells: a new fate for differentiating helper T cells. *Immunol Res.* 2008;41:87-102.
14. Noack M, Miossec P. Th17 and regulatory T cell balance in autoimmune and inflammatory diseases. *Autoimmun Rev.* 2014;13:668-77.

15. Kryczek I, Wei S, Vatan L, Escara-Wilke J, Szeliga W, Keller ET, et al. Cutting edge: opposite effects of IL-1 and IL-2 on the regulation of IL-17<sup>+</sup> T cell pool IL-1 subverts IL-2-mediated suppression. *J Immunol*. 2007;179:1423-6.
16. Nurieva R, Yang XO, Martinez G, Zhang Y, Panopoulos AD, Ma L, et al. Essential autocrine regulation by IL-21 in the generation of inflammatory T cells. *Nature*. 2007;448:480-3.
17. Postigo J, Iglesias M, Álvarez P, Augustin JJ, Buelta L, Merino J, et al. Bone morphogenetic protein and activin membrane-bound inhibitor, a transforming growth factor  $\beta$  rheostat that controls murine Treg cell/Th17 cell differentiation and the development of autoimmune arthritis by reducing interleukin-2 signaling. *Arthritis Rheumatol*. 2016;68:1551-62.
18. Onichtchouk D, Chen YG, Dosch R, Gawantka V, Delius H, Massagué J, et al. Silencing of TGF- $\beta$  signaling by the pseudoreceptor BAMBI. *Nature*. 1999;401:480-5.
19. Uyttenhove C, Sommereyns C, Théate I, Michiels T, Van Snick J. Anti-IL-17A autovaccination prevents clinical and histological manifestations of experimental autoimmune encephalomyelitis. *Ann N Y Acad Sci*. 2007;1110:330-6.
20. Khmaladze I, Kelkka T, Guerard S, Wing K, Pizzolla A, Saxena A, et al. Mannan induces ROS-regulated, IL-17A-dependent psoriasis arthritis-like disease in mice. *Proc Natl Acad Sci USA*. 2014;111:E3669-78.
21. Postigo J, Genre F, Iglesias M, Fernández-Rey M, Buelta L, Rodríguez-Rey JC, et al. Exacerbation of type II collagen-induced arthritis in apolipoprotein E-deficient mice in association with the expansion of Th1 and Th17 cells. *Arthritis Rheum*. 2011;63:971-80.
22. Boyman O, Kovar M, Rubinstein MP, Surh CD, Sprent J. Selective stimulation of T cell subsets with antibody-cytokine immune complexes. *Science*. 2006;311:1924-27.
23. Mabuchi T, Singh TP, Takekoshi T, Jia GF, Wu X, Kao MC, et al. CCR6 is required for epidermal trafficking of  $\gamma\delta$ -T cells in an IL-23-induced model of psoriasiform dermatitis. *J Invest Dermatol*. 2013;133:164-71.
24. Tramullas M, Lantero A, Díaz A, Morchón N, Merino D, Villar A, et al. BAMBI (bone morphogenetic protein and activin membrane-bound inhibitor) reveals the involvement of the transforming growth factor-beta family in pain modulation. *J Neurosci*. 2010;30:1502-11.
25. Lin Z, Gao C, Ning Y, He X, Wu W, Chen YG. The pseudoreceptor BMP and activin membrane-bound inhibitor positively modulates Wnt/beta-catenin signaling. *J Biol Chem*. 2008;283:33053-8.



26. Nakajima K, Sano S. Mouse models of psoriasis and their relevance. *J Dermatol.* 2018;45:252-63.
27. Singh TP, Zhang HH, Hwang ST, Farber JM. IL-23- and imiquimod-induced models of experimental psoriasis in mice. *Curr Protoc Immunol.* 2019:e71.
28. Koreth J, Matsuoka K, Kim HT, McDonough SM, Bindra B, Alyea EP3rd, et al. Interleukin-2 and regulatory T cells in graft-versus-host disease. *N Engl J Med.* 2011;365:2055-66.
29. Matsuoka K, Koreth J, Kim HT, Bascug G, McDonough S, Kawano Y, et al. Low-dose interleukin-2 therapy restores regulatory T cell homeostasis in patients with chronic graft-versus-host disease. *Sci Transl Med.* 2013;5:179ra43.
30. Saadoun D, Rosenzweig M, Joly F, Six A, Carrat F, Thibault V, et al. Regulatory T-cell responses to low-dose interleukin-2 in HCV-induced vasculitis. *N Engl J Med.* 2011;365:2067-77.
31. Neuberger MS, Rajewsky K. Activation mouse complement by monoclonal mouse antibodies. *Eur J Immunol.* 1981;11:1012-6.
32. Lande R, Gregorio J, Facchinetti V, Chatterjee B, Wang YH, Homey B, et al. Plasmacytoid dendritic cells sense self-DNA coupled with antimicrobial peptide. *Nature.* 2007;449:564-9.
33. Ganguly D, Chamilos G, Lande R, Gregorio J, Meller S, Facchinetti V, et al. Self-RNA-antimicrobial peptide complexes activate human dendritic cells through TLR7 and TLR8. *J Exp Med.* 2009;206:1983-94.
34. Lowes MA, Suárez-Fariñas M, Krueger JG. Immunology of psoriasis. *Annu Rev Immunol.* 2014;32:227-55.
35. Stockenhuber K, Hegazy AN, West NR, Ilott NE, Stockenhuber A, Bullers SJ, et al. Foxp3<sup>+</sup> T reg cells control psoriasiform inflammation by restraining an IFN-I-driven CD8<sup>+</sup> T cell response. *J Exp Med.* 2018;215:1987-98.
36. Hartwig T, Zwicky P, Schreiner B, Yawalkar N, Cheng P, Navarini A, et al. Regulatory T cells restrain pathogenic T helper cells during skin inflammation. *Cell Rep.* 2018;25:3564-72.
37. Kim J, Krueger JG. Highly effective new treatments for psoriasis target the IL-23/type 17 T cell autoimmune axis. *Annu Rev Med.* 2017;68:255-69.
38. Reiss M, Sartorelli AC. Regulation of growth and differentiation of human keratinocytes by type beta transforming growth factor and epidermal growth factor. *Cancer Res.* 1987;47:6705-9.

39. Mansbridge JN, Hanawalt PC. Role of transforming growth factor beta in the maturation of human epidermal keratinocytes. *J Invest Dermatol.* 1988;90:336-41.
40. Doi H, Shibata MA, Kiyokane K, Otsuki Y. Downregulation of TGFbeta isoforms and their receptors contributes to keratinocyte hyperproliferation in psoriasis vulgaris. *J Dermatol Sci.* 2003;33:7-16.
41. Elango T, Thirupathi A, Subramanian S, Dayalan H, Gnanaraj P. Methotrexate normalized keratinocyte activation cycle by overturning abnormal keratins as well as deregulated inflammatory mediators in psoriatic patients. *Clin Chim Acta.* 2015;451:329-37.
42. Flisiak I, Chodynicka B, Porebski P, Flisiak R. Association between psoriasis severity and transforming growth factor beta(1) and beta (2) in plasma and scales from psoriatic lesions. *Cytokine.* 2002;19:121-5.
43. Li AG, Wang D, Feng XH, Wang XJ. Latent TGFbeta1 overexpression in keratinocytes results in a severe psoriasis-like skin disorder. *EMBO J.* 2004;23:1770-81.
44. Han G, Williams CA, Salter K, Garl PJ, Li AG, Wang XJ. A role for TGFbeta signaling in the pathogenesis of psoriasis. *J Invest Dermatol.* 2010;130:371-7.
45. Mohammed J, Ryscavage A, Perez-Lorenzo R, Gunderson AJ, Blazanin N, Glick AB. TGFbeta1-induced inflammation in premalignant epidermal squamous lesions requires IL-17. *J Invest Dermatol.* 2010;130:2295-303.
46. Rosman Z, Shoenfeld Y, Zandman-Goddard G. Biologic therapy for autoimmune diseases: an update. *BMC Medicine.* 2013;11:88.
47. Moroncini G, Calogera G, Benfaremo D, Gabrielli A. Biologics in inflammatory immune-mediated systemic diseases. *Curr Pharm Biotechnol.* 2017;18:1008-16.
48. Weinblatt ME, Kremer JM, Bankhurst AD, Bulpitt KJ, Fleischmann RM, Fox RI, et al. A trial of etanercept, a recombinant tumor necrosis factor receptor:Fc fusion protein, in patients with rheumatoid arthritis receiving methotrexate. *N Engl J Med.* 1999;340:253-9.
49. Tavakolpour S, Darvishi M, Ghasemiadl M. Pharmacogenetics: A strategy for personalized medicine for autoimmune diseases. *Clin Genet.* 2018;93:481-97.

## Figure Legends

**Figure 1: Effects of BAMBI inhibition in the in vivo IL-2 IC-induced expansion and in vitro regulatory activity of Tregs.** (A) IgG1-C- (○) or B101.37-treated (●) B6.WT and B6.BAMBI-KO (▲) 2 month-old mice were injected ip with PBS or with 6 μg JES6-1A12 containing IL-2 IC during 3 consecutive days. Percentages of Tregs in lymph nodes and spleen of individual mice were evaluated 5 days later by flow cytometry. (B) Expression levels of CD25 in Tregs from IgG1-C- (○) or B101.37-treated (●) B6.WT and B6.BAMBI-KO (▲) mice after injection of PBS or JES6-1A12 containing IL-2 IC. Mean fluorescence intensity (MFI) values in individual mice are expressed. (C) Effect of in vitro BAMBI inhibition with B143.14 mAb in Treg activity. Different ratios of naïve CD4<sup>+</sup>CD25<sup>-</sup>/Treg cells from B6.WT mice were stimulated with anti-CD3 antibodies in the presence of B6.WT APCs and polyclonal IgM (○) or B143.14 mAb (●). Cumulative results of 3 independent experiments are expressed as the mean ± SD of the incorporation of <sup>3</sup>H-TdR in triplicate cultures. Statistical differences were analyzed by Student's t-test (A and B) and by two-way ANOVA and Sidak's multiple comparison test (C) as follows: \*p<0.05, \*\*p<0.01 and \*\*\*p<0.001.

**Figure 2: Development of MIP after BAMBI deficiency or inhibition with B101.37 mAb.** Mice were injected with 10 mg of SCM. (A) Kinetics (mean ± SD; n= 5-7 mice/group) of skin psoriasis (left panel) and paw swelling (right panel). Representative macroscopic (upper panels) and histological skin lesions (x10 lower panels) (B) or macroscopic paw swelling (C). (D) Cytokine expression in the ears (upper panels) and hind paws (lower panels) of mice 6 days after PBS of SCM injection, analyzed by quantitative real-time RT-PCR. Cumulative results are expressed as mean ± SD fold change (n= 7-9 mice/group) of each cytokine relative to GAPDH expression. (E) Percentages of Tregs (upper panels) and T<sub>H</sub>17 cells (lower panels) in individual mice in lymph nodes and spleen determined by flow cytometry. (F) Dot plots and mean values of CD4<sup>+</sup>IL-17<sup>+</sup> (upper plots) and CD4<sup>+</sup>FoxP3<sup>+</sup> (lower plots) cells in a representative ear cell pool. (G) Percentages of Tregs (left) and T<sub>H</sub>17 cells (right) in individual ear cell pools. Statistical differences were analyzed by two-way ANOVA and Sidak's multiple comparison test (A), Student's t test (D) and one-way ANOVA with Tukey's multiple comparison (E) and indicated as follows: \*p<0.05, \*\*p<0.01 and \*\*\* p<0.001.

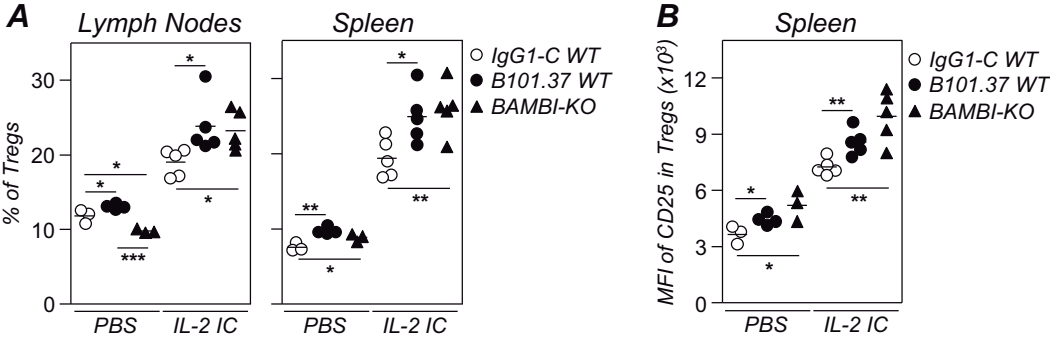
**Figure 3: Treg- and TGF $\beta$ -dependent protection against MIP after BAMBI deficiency or its pharmacological inhibition with B101.37 mAb.** (A) Schematic representation of BMC chimeras. (B) Kinetics of skin psoriasis (left) and paw swelling (right) development in chimeras in two independent experiments. Results are expressed as the mean  $\pm$  SD (n= 3-6 mice/group). (C, D) Two-three months-old B10RIII.BAMBI-KO (C) and IgG1-C- or B101.37-treated WT mice (D) depleted or not in CD4<sup>+</sup>CD25<sup>+</sup> Tregs (upper panels) or after treatment with anti-TGF $\beta$  mAb (lower panels) received a single injection of 10 mg of SCM. Kinetics of skin psoriasis (left panel) and paw swelling (right panel) development. Results are expressed as the mean  $\pm$  SD (n= 4-6 mice/group). (E) IgG1-C- or B101.37-treated B10RIII.WT and BAMBI-KO and mice depleted or not in CD4<sup>+</sup>CD25<sup>+</sup> Tregs and treated or not with anti-IL-17A mAb received a single injection of 10 mg of SCM. Severity of skin psoriasis (left panel) and paw swelling (right panel) in individual mice 6 days after SCM injection. Statistical differences were analyzed by two-way ANOVA, with Tukey's (B) or Dunnett's (C and D) multiple comparison test and by Student's t test (E) and indicated as follows: \*p<0.05, \*\*p<0.01 and \*\*\* p<0.001.

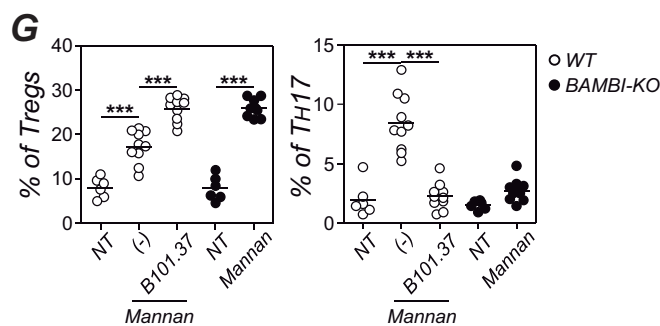
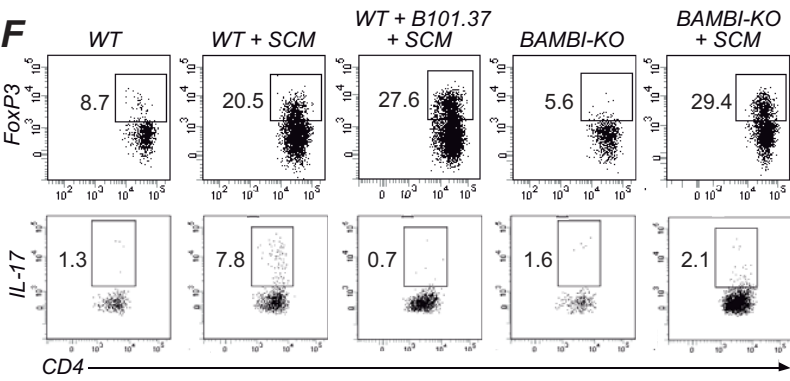
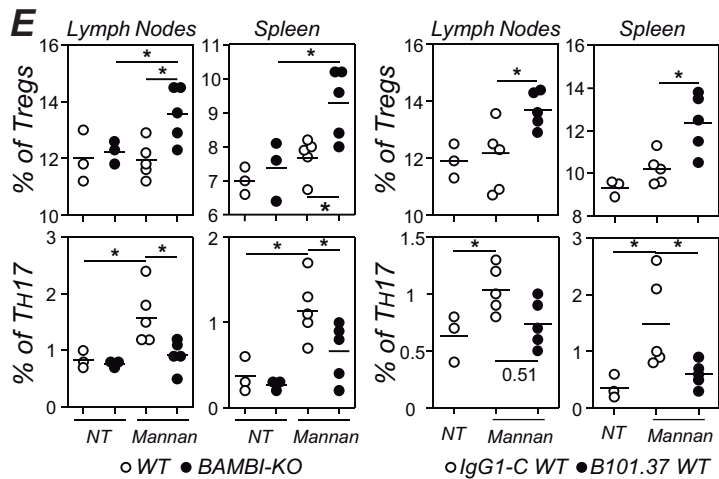
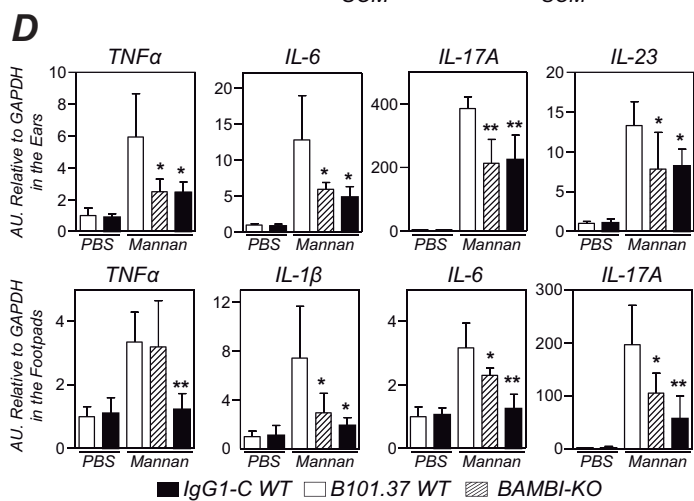
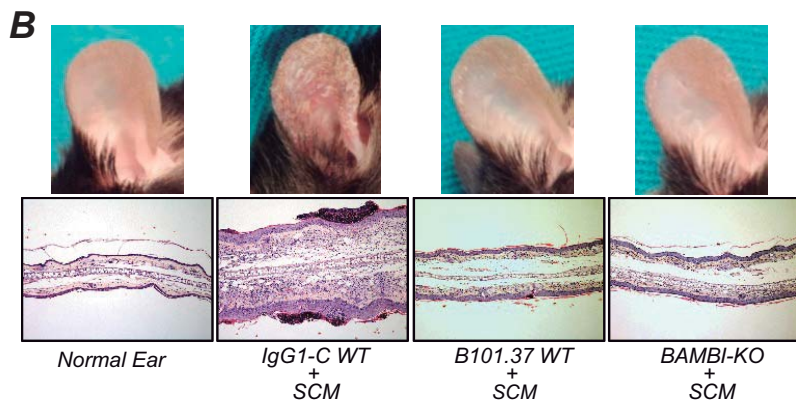
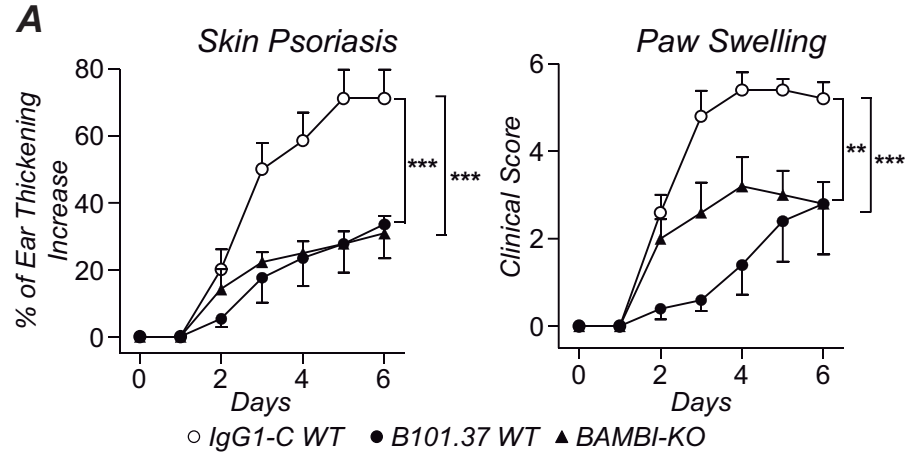
**Figure 4: Preventive and therapeutic effects of B101.37 treatment in MIP.** Two-three month-old B10RIII WT mice that received weekly injections of 10 mg of SCM (black arrows) were treated with 2 mg/week of IgG1-C ( $\circ$ ) or with B101.37 mAb in preventive ( $\bullet$ ; starting at the time of the first SMC injection) or therapeutic ( $\Delta$ ; starting 3 days after SCM injection; white arrow) protocols. An additional group received a single dose of mAbs at the time of SMC injection ( $\blacktriangle$ ). Kinetics of skin psoriasis (upper panel) and paw swelling (lower panel) development, expressed as the mean  $\pm$  SD (n= 5-7 mice/group), in two independent experiments. Statistical differences were analyzed by two-way ANOVA with Dunnett's multiple comparison test and indicated as follows: \*p<0.05, \*\*p<0.01 and \*\*\* p<0.001.

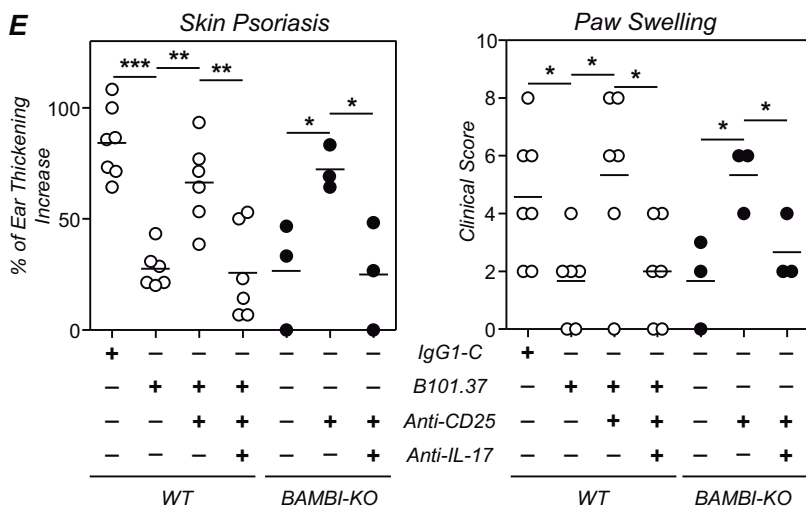
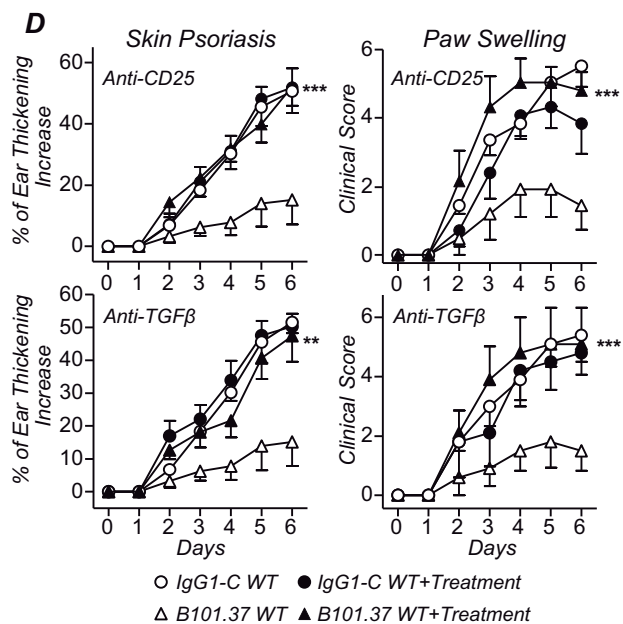
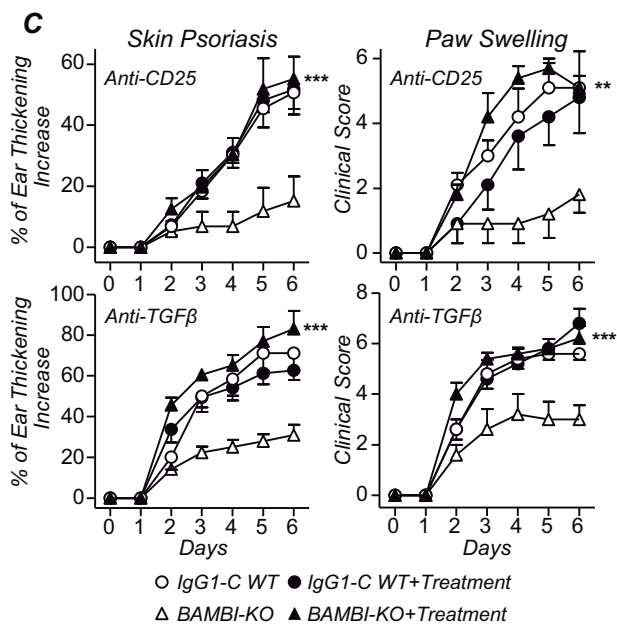
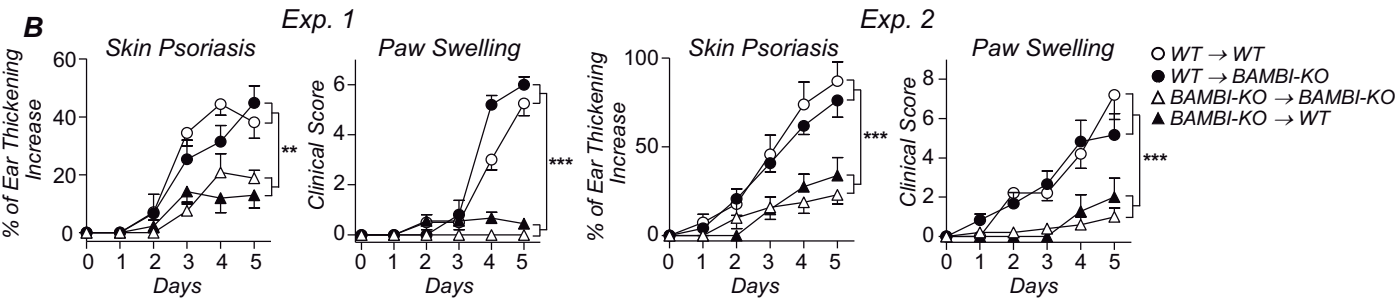
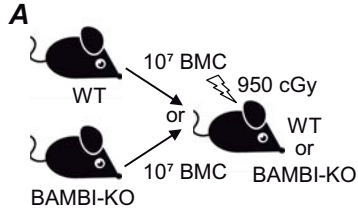
**Figure 5: Effects of BAMBI deficiency or treatment with B101.37 mAb in imiquimod-induced psoriasis.** Two-three month-old IgG1-C- or B101.37-treated B10RIII.WT and BAMBI-KO mice received topical applications of a cream containing 5% imiquimod for five consecutive days (12.5 mg imiquimod/day) in the right ears. Left ears were kept untreated as controls. (A) Kinetics of skin psoriasis development. Results are expressed as the mean  $\pm$  SD (5-7 mice/group). (B) Representative histological skin lesions ( $\times 10$  lower panels) of mice depicted in (A). (C) Epidermal and dermal thickening quantification in individual mice ( $\mu\text{m}$ ) in imiquimod-treated

ears. Statistical differences were analyzed by two-way ANOVA with Dunnett's multiple comparison test (A) and Student's t test (C) and indicated as follows: \* $p < 0.05$ , \*\* $p < 0.01$  and \*\*\* $p < 0.001$ .

**Figure 6: Effects of BAMBI deficiency or treatment with B101.37 mAb in CIA.** Two-three months-old IgG1-C- or B101.37-treated B10RIII.WT and BAMBI-KO mice were immunized with col II-CFA. (A) Kinetic of arthritis severity (left panel) expressed as the mean  $\pm$  SD and arthritis severity in individual mice 8 weeks after immunization (right panel). (B) Representative radiological images (upper panels) and extent of individual radiological signs (lower panels), expressed as the mean  $\pm$  SD (n= 7-8 mice/group), 8 weeks after immunization. (C) Representative histological images (left panels) and histological score in individual mice (right panel). Statistical differences were analyzed by two-way ANOVA with Dunnett's multiple comparison test (A) and Student's t test (A-C) and indicated as follows: \* $p < 0.05$ , \*\* $p < 0.01$  and \*\*\* $p < 0.001$ .

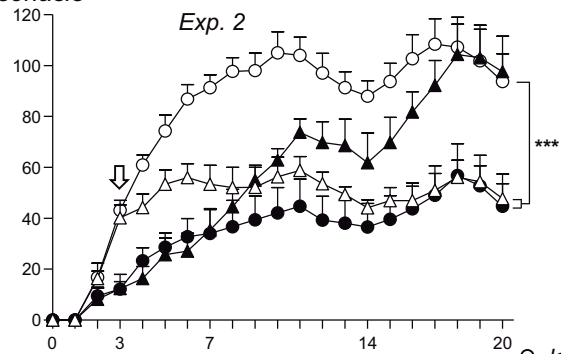
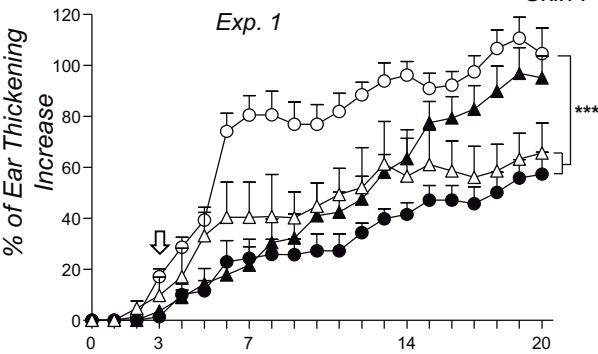








### Skin Psoriasis



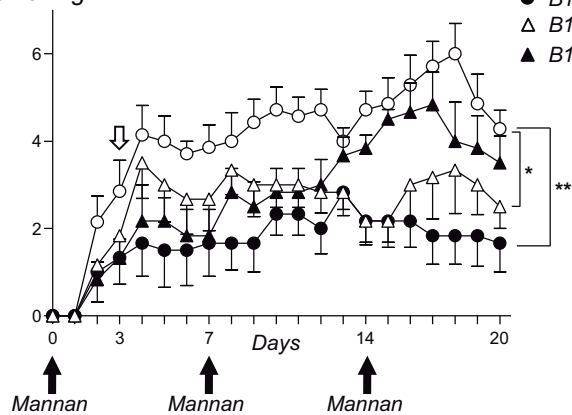
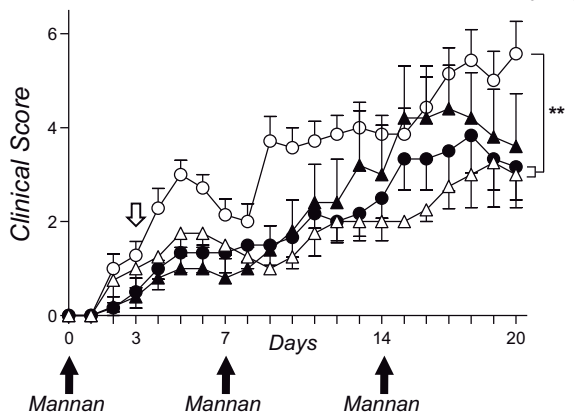
○ IgG1-C WT

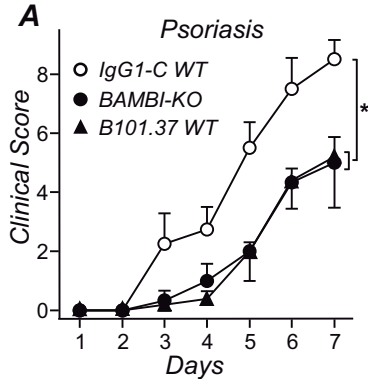
● B101.37 WT (preventive)

△ B101.37 WT (therapeutic)

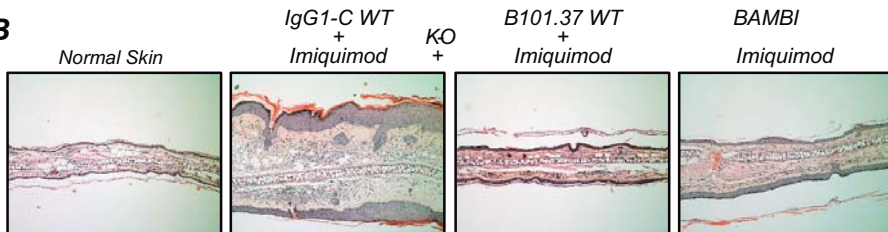
▲ B101.37 WT (single dose)

### Paw Swelling





**B**



**C**

